COMPOSITE INTERFACES
https://doi.org/10.1080/09276440.2021.1913901

Taylor & Francis
Taylor & Francis Group

ARTICLE

OPEN ACCESS Check for updates

Characterization of interfacial strength in natural fibre – polyolefin composites at different temperatures

James L. Thomason [a] and Jose L. Rudeiros-Fernández [a,b]

[a]University of Strathclyde, Department of Mechanical and Aerospace Engineering, Glasgow UK; [b]Lawrence Berkeley National Laboratory, Berkeley, CA United States

ABSTRACT

It is often suggested that optimization of the fibre-matrix interfacial adhesion is essential to improve the mechanical performance of natural fibre reinforced thermoplastic compounds. The use of such composites in many applications often requires characterisation of performance over a range of temperatures. This paper presents a study on the measurements of the interfacial adhesion of coir fibre with various polyolefin matrices at room temperature. We then present a novel adaptation of a dynamical mechanical analyser to enable the measurement of interfacial shear strength over the temperature range of −40°C to 120°C. Results from these measurements are presented and discussed in terms of the relationship of apparent IFSS to residual thermal stresses in such thermoplastic composites.

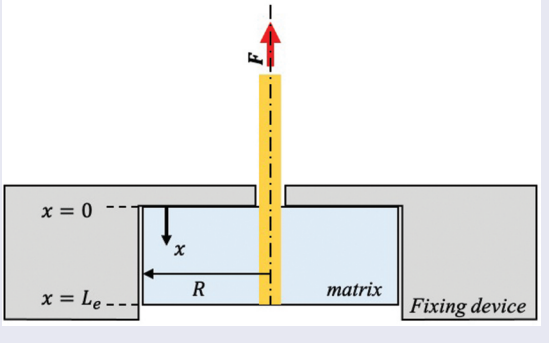

ARTICLE HISTORY
Received 19 January 2021
Accepted 5 April 2021

KEYWORDS
Natural fibres; interface/interphase; thermoplastic composites; interfacial shear strength

1. Introduction

During the last decades, natural fibres (NF), considered to be an environmentally sustainable alternative to some human-made fibres and mineral fillers, have been increasingly proposed for use as reinforcements in composite materials [1–3]. Aspects such as governmental environmental regulations, and increasing social awareness of sustainability, have been driving the increasing interest of these 'green' materials, and particularly natural fibre reinforced polymer matrix composites. However, despite the

CONTACT James L. Thomason james.thomason@strath.ac.uk University of Strathclyde, Department of Mechanical and Aerospace Engineering, Glasgow UK

potential of this kind of composite, especially with regard to natural fibre reinforced thermoplastics composites (NFTC), different issues in relation to their performance and technical applicability have to be resolved before their implementation on a larger industrial scale [4–8].

In relation to the mechanical properties of natural fibres, one of the critical aspects of their use as reinforcement in thermoplastics, is the risk of fibre degradation at high thermoplastic processing temperatures [6,9]. In this regard, there is a clear limitation in the number of thermoplastics that can be used for NFTCs. Thermo-mechanical degradation influences the performance of, generally negatively, and it is crucial to understand their behaviour at composite processing temperature conditions. Natural fibres are usually polar, having inherently low compatibility with non-polar matrices, such as polypropylene (PP) and polyethylene (PE) [10]. For this reason, in order to fully exploit their potential in NFTCs, it is necessary to enhance the stress transfer capability of the fibre–matrix interface [3,6–8]. Established treatments, such as maleic anhydride grafted polyolefins or silane modifications, normally applied for human-made mineral/inorganic fibres, have not been as successful in NFTCs [3,8,11,12]. Consequently, a deeper understanding of the fibre-matrix interfacial behaviour, including the dependency of apparent properties on the geometry of the fibre and of the samples, is a fundamental requirement.

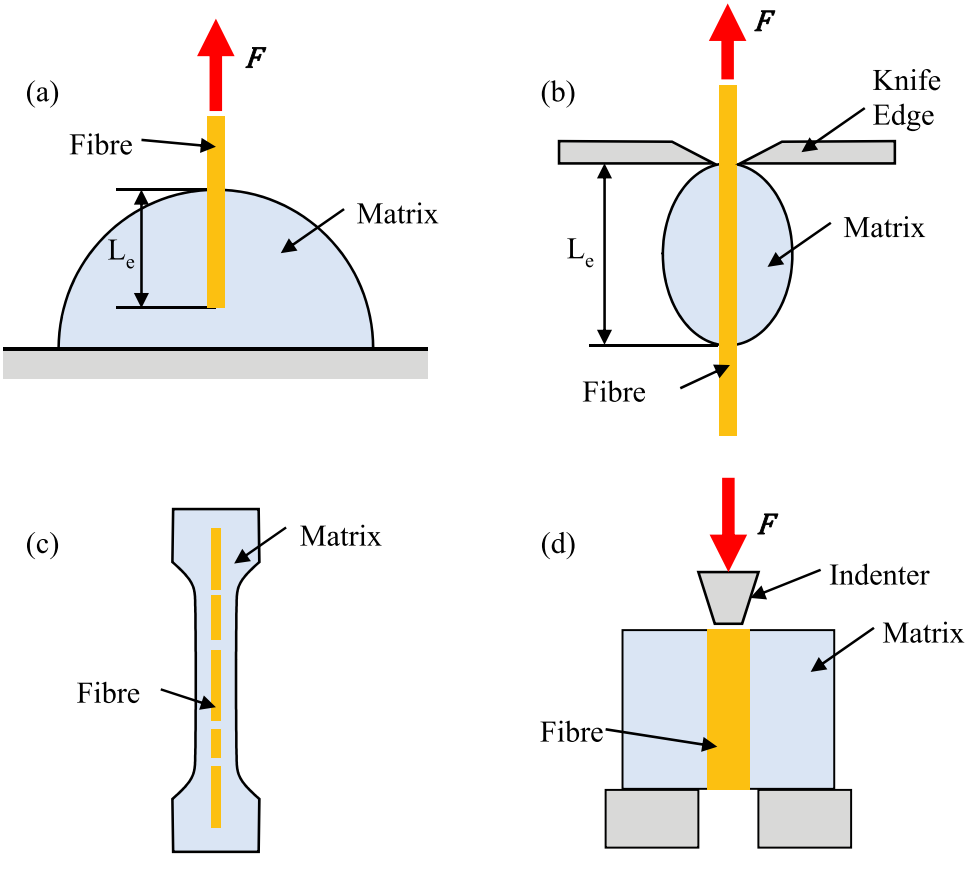

Figure 1. Micromechanical tests: (a) pull-out, (b) microbond, (c) fragmentation, and push-out.

Moreover, understanding the relationship between fibre, matrix and interfacial properties, and NFTCs performance is vital, as it should provide clear insights into potential routes for improvement.

The nature of interfacial bonding influences the elastic and fracture properties of the composite in different ways [13]. When analysing fibre reinforced composites, single-fibre experiments are normally used to investigate the interfacial bond strength. These micromechanical tests include four main categories: pull-out, microbond, fragmentation, and push-out as illustrated in Figure 1. However, the direct measurement of interfacial properties often relies on many assumptions which can potentially lead to serious inaccuracies. The parameters that can affect the results of such interfacial measurements have been extensively discussed in the literature [14–25]. These include fibre diameter, embedded length, geometrical loading configuration or symmetry of the specimen. Moreover, most of these types of measurements involve shear debonding and consequent sliding. However, an interface exhibiting high shear debonding stress may not necessarily exhibit strong normal debonding stress. Therefore, it is necessary to take into consideration this factor when relating interfacial data to macroscopic composite behaviour. Furthermore, the fact that these tests are carried out in artificial single-fibre composites, which do not include neighbour fibres, may also lead to different results.

In the case of characterising the interface in NF composites there are a number of challenges to be considered when choosing which of these techniques to use. The pushout test relies on the internal structure of the fibre being robust enough to transmit the stress applied by the indentor uniformly across the fibre cross-section. However, the weak internal structure of NFs is well known and would be suspect in this technique. Furthermore, the samples for the push-out test require polishing (often on both sides). The high level of moisture sensitivity of NFs could very probably lead to major changes in fibre and interface properties during such polishing. For these reasons the push-out test was not selected in this investigation.

A major requirement for a useful interpretation of the fragmentation test results is the ability to obtain a very accurate characterisation of the fibre tensile strength at a range of gauge lengths in order to extrapolate a value of fibre strength at the short gauge length obtained during the multiple fracture of the single test fibre. This requirement is already a challenge for those employing this test method on man-made fibres. However, in this context NF present further major challenges in terms of the very high variability of many fibre parameters such as cross-section shape and area, surface roughness, uniformity of cross-section along the test gauge length, linearity of fibre shape, and of course, the varying individual internal structure of each fibre which determines load at failure. It is considered that these major experimental challenges immediately preclude the use of the fragmentation test for interface characterisation in NF composites. This leaves the two test methods which involve pulling an embedded single fibre out of a sample of the polymer matrix. The microbond test is often used in fibre-matrix combinations with high levels of adhesion which necessitate very short embedded lengths if the failure mode is to be interfacial failure and not fibre tensile failure. Given the low levels of expected adhesion strength in NF composites it was not deemed necessary to use this test method. Moreover, initial exploration of microbond sample preparation using coir fibres indicated that the yield of axisymmetric droplets on the fibres (a necessary condition of the

microbond test) was very low. This was possibly due to the much larger and irregular diameter of coir fibres in comparison the carbon and glass fibres used in the development of the microbond test.

Hence, by the above process of elimination, we arrive at the single fibre pullout test as the preferred method for micromechanical testing of interfacial strength in the coir-PP system. In order to obtain useful interfacial strength results using this test method it is still necessary to overcome a number of experimental challenges in both sample preparation, test setup, and data analysis. These include

- Fibre degradation at PP processing temperatures
- PP degradation in the preparation of small-scale samples
- Accurate characterisation of the non-circular fibre perimeter (for the calculation embedded area)
- Test sample preparation with curved fibres
- Sample mounting jigs for using in tensile testing
- Accurate control of testing environment for measurement of temperature dependence of interface strength
- Data reduction method to obtain interface parameters from load displacement curves obtain in testing

In this paper, we describe methods which have been developed to overcome these issues to enable useful values for the interfacial shear strength (IFSS) of the coir-PP system to be obtained by single fibre pullout (SFP) testing.

Figure 2. Coir fibres as received.

2. Materials and methods

2.1 Materials

The coir fibre and polymers used for this study were provided by SABIC (Geleen, the Netherlands). Coir fibres were used as delivered for pull-out testing. An example of the highly curved and coiled nature of the coir fibres is shown in Figure 2 where the wide range of fibre diameters can also be observed. The matrices used for composites and pull-out testing were homopolymer (hPP) polypropylene 579S with melt flow index (MFI) of 47 g/10 min, and copolymer (cPP) polypropylene 513MNK10 with MFI 70 g/10 min. Maleic anhydride grafted polypropylene (MaPP) Exxelor PO 1020 (density 0.9 g/cm^3 and melt flow index 430 g/10 min at 230°C, 110 g/10 min at 190°C) with a 'very high' maleic anhydride content range (0.5 to 1%) was used to enhance interfacial interaction in hPP samples. In the case of LDPE, 1922SF, with a MFI (190°C and 2.16 Kg) of 22 g/10 min was used. Maleic anhydride modified high-density polyethylene (MaPE) Polybond 3029 (density 0.95 g/cm^3 and melt flow index 4 g/10 min at 190°C) with a 'very high' maleic anhydride content range (1.5 to 1.7%) was used to enhance interfacial interaction in LDPE samples.

2.2 Sample preparation

As illustrated in Figure 1 the SFP test requires samples with a single fibre embedded in a block of polymer. The aim in this work was to create a pull-out sample with similar geometrical configuration to the idealised sample proposed by Scheer and Nairn [23], illustrated in Figure 3. In this pull-out configuration, a cylindrical sample, in which a fibre is embedded along the central axis of the cylinder, is restrained on the top surface of the

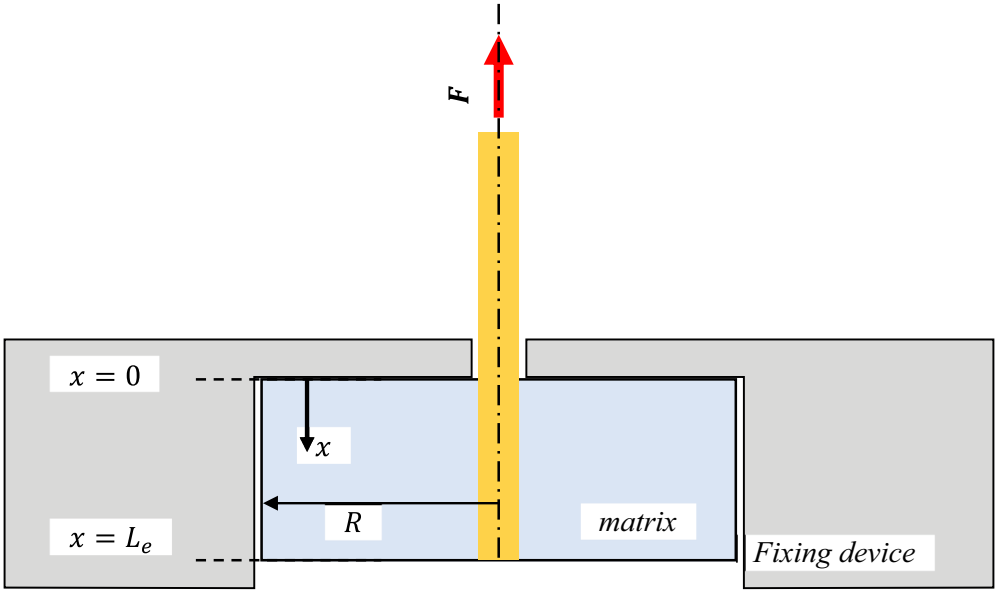

Figure 3. Cylindrical pull-out sample in the pull-out configuration.

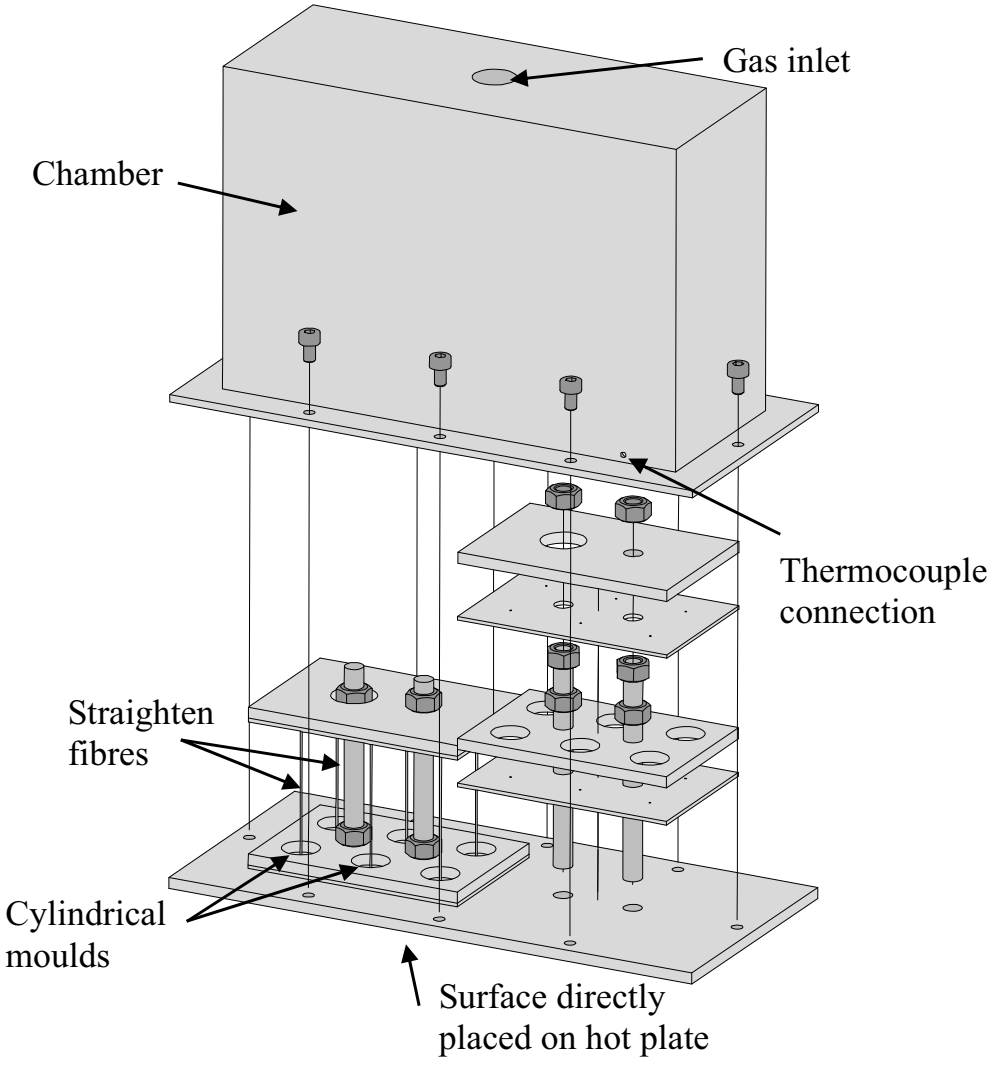

Figure 4. General diagram of the sample preparation frame.

cylinder. Yang and Thomason have reported the absolute necessity of preparing PP-based samples for micromechanical testing in an inert atmosphere to avoid major errors that can be obtained due to thermo-oxidative degradation of the PP [26]. Since degradation of NF is also an issue at PP processing temperatures, the sample preparation methodology had to involve maintaining the process under an inert atmosphere. The sample preparation technique also had to take into consideration the high curvature and diameter variability of coir fibres, which is illustrated in Figure 2.

The method and jigs developed for sample preparation methods are illustrated in Figures 4 and Figures 5. Fibres are held straight in the jig with the help of a metal frame, which has a series of 10 mm diameter cylindrical moulds for melting typical polymer pellets into cylindrical blocks in which the fibres are embedded. In the first step fibres were threaded through holes on plate 1, and thereafter fixed on the underside of the plate

Figure 5. Metal frame and chamber with the gas connection.

with double sided tape, as shown in Figure 6 (a). Once all the fibres were threaded through the respective holes in the plate, it was placed on the base plate, which provided additional gripping of the fibres, Figure 6 (b). These actions were repeated for the second plate 1, providing 12 individual samples in total. Thereafter, the two plates with the cylindrical moulds were put through the fibres and located on top of plates 1. The mould plates were compressed against the base plate with the help of two nuts mounted on perpendicular threaded bars, which are directly screwed in the base plate.

Once this operation was completed, the fibres were threaded through the holes of the second plate (plate 2), and once they are perfectly straight between both plates (i.e. the

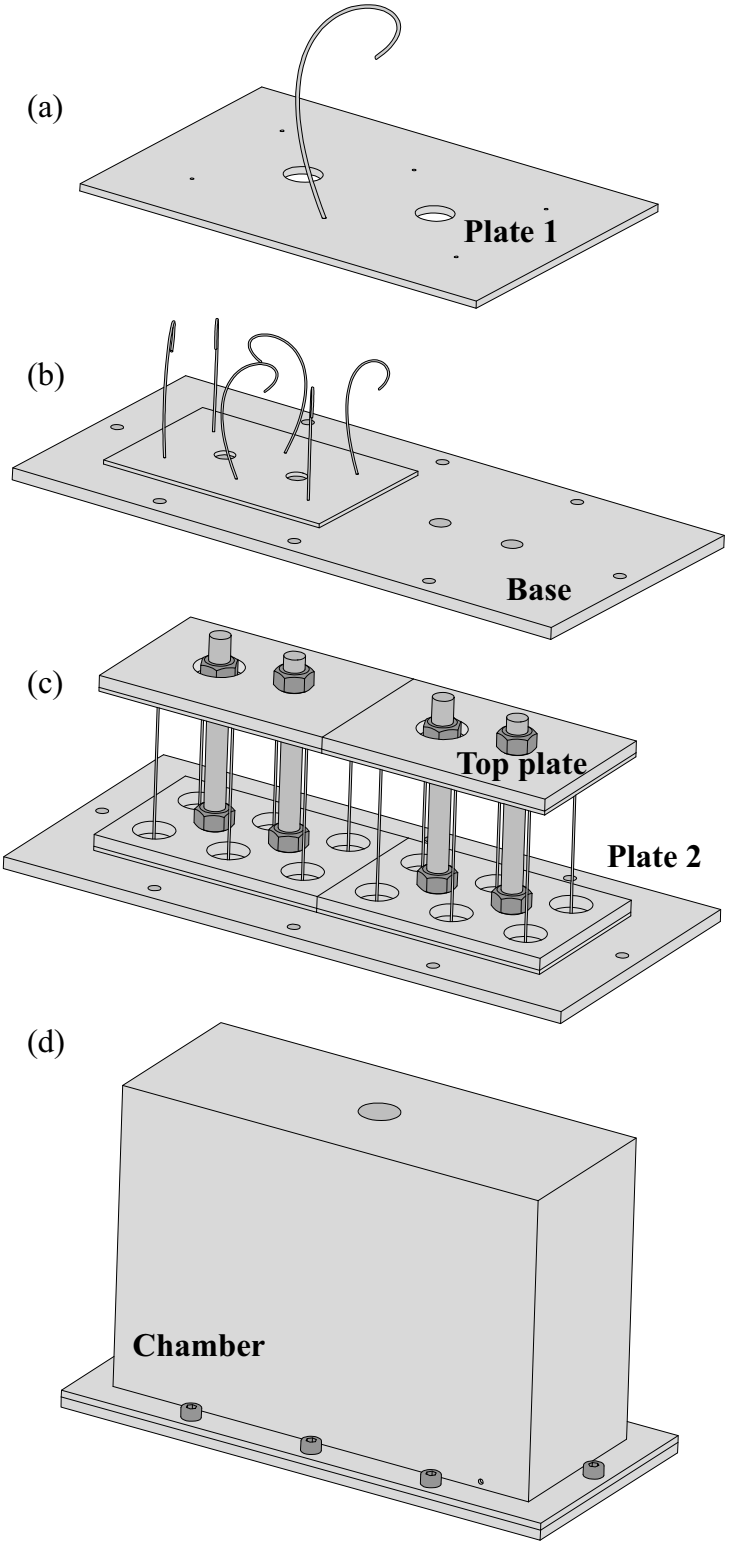

Figure 6. Pull out sample preparation schematic sequence.

fibres were perpendicular to the planes represented by plate 1 and plate 2), they were fixed with double-sided tape. Both plates 2 were supported and fixed by nuts on the threaded bars. Thereafter, two additional plates were compressed against plates 2 for additional gripping of the fibres, as can be seen in Figure 6(c). At this point, the cylindrical mould cavities were filled with polymer pellets. The assembly was then enclosed in its chamber, which is fixed directly to the base, as shown in Figure 6 (d). A thermocouple wire and the gas inlet were then connected to the chamber and the chamber was flushed with dry nitrogen.

In order to melt the pellets, the base of the assembly was placed directly on the surface of a hot plate pre-heated to 230°C. The total time that the assembly was placed on the hot plate was fixed at 18 minutes for PP and PE samples, which was found to be enough to completely melt the polymers. The temperature in the base plate, which is in direct contact with the polymer pellets reached a maximum temperature of approximately 200° C, after 18 minutes on the hot plate, as illustrated in Figure 7. However, it can also be noted in this Figure that the temperature of the nitrogen atmosphere surrounding the fibres remained below 150°C which significantly reduced the likelihood of degradation of the coir fibre [9,27].

After the 18 minutes, the assembly was removed from the hot plate and allowed to cool down at room temperature at which point the parts can be disassembled. The fibres were cut next to the points where they were fixed by the double-sided tape which then allowed for easy demoulding of the cylindrically shaped polymer samples. Thereafter, the remaining part of the fibre below the polymer block was removed with a scalpel. Additionally, any sharp edges in the outer cylinder face were also removed with a scalpel. An example of the samples produced is shown in Figure 8.

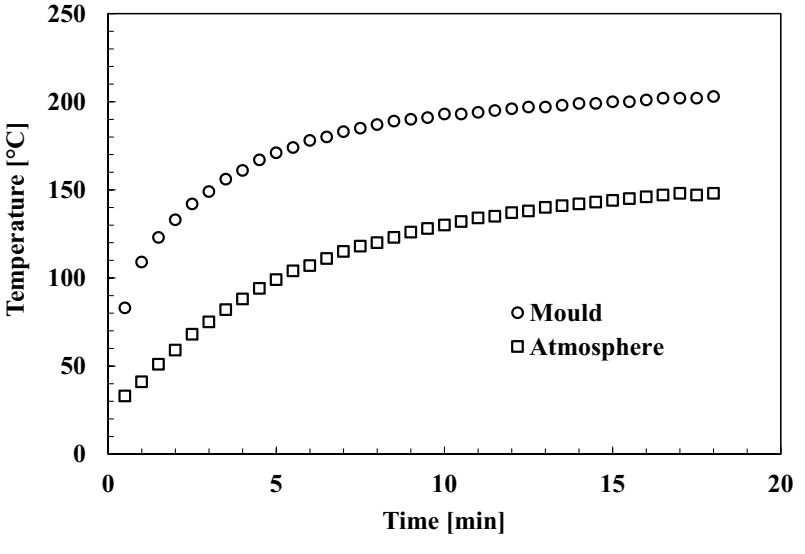

Figure 7. Evolution of the temperature of the mould and chamber atmosphere versus time for the hot plate at 230°C with a N2 flow of 200 ml/min.

Figure 8. Example of typical Coir-PP cylindrical pull-out samples.

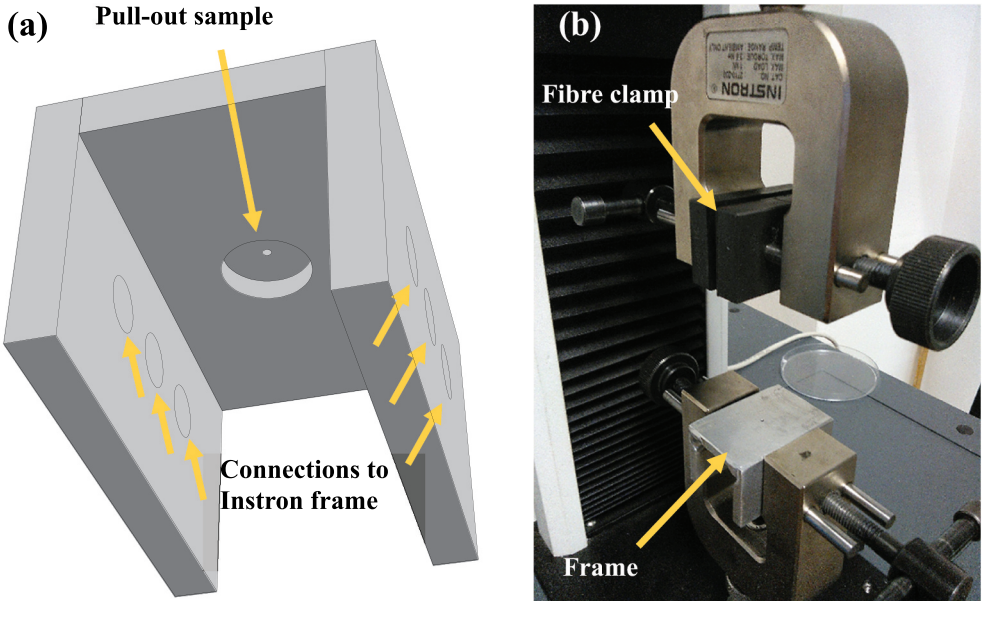

Figure 9. Instron pull-out frame. (a) Schematic drawing of the frame. (b) Instron set-up.

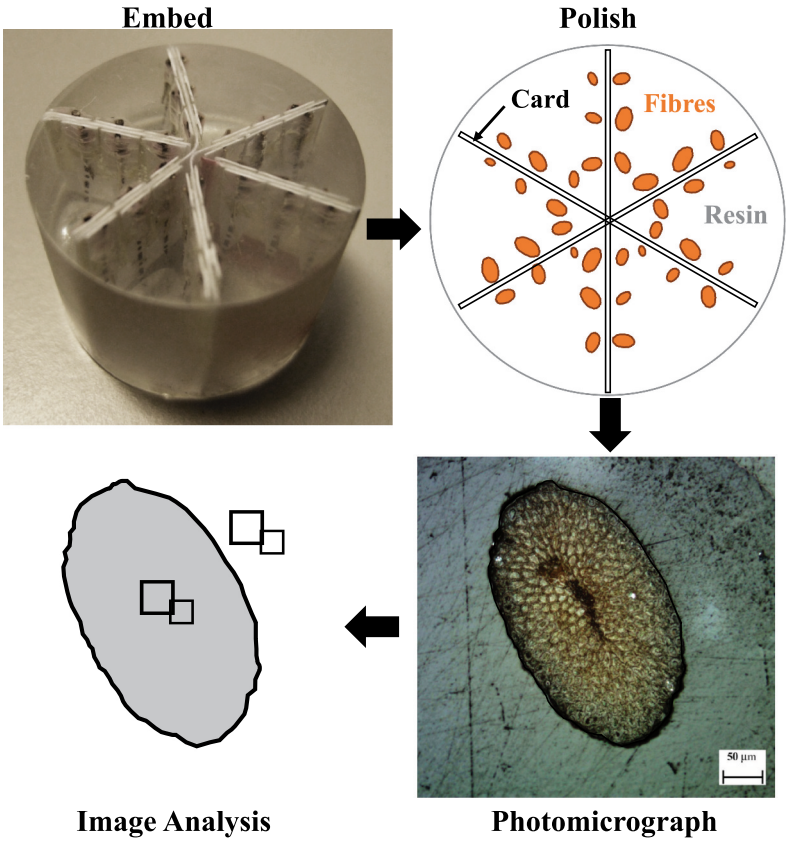

Figure 10. Process of determining the CSA (A_f) and perimeter (P_f) of natural fibre samples.

2.3 Room temperature single fibre pull-out test

A cylindrical fixing device was manufactured, illustrated in Figure 9, to be fitted to the main frame of an Instron 3342 tensile testing machine, which was used for the pull-out testing. A 100 N load cell was used for the measurements. After positioning the pull-out samples in the frame as showed in Figure 9, fibres were clamped at approximately 5 mm above the top surface of the pull-out frame, which resulted on a total free length of approximately 7 mm. Fibres were pulled at a cross-head displacement rate of 0.5 mm/min.) Load-displacement curves were recorded using Bluehill2 Software and post-processed to find the peak load (F_{max}). Subsequently, the peak load, fibre perimeter (P_f) and embedded length (L_e) were used to calculate the apparent IFSS (τ_{app}).

$$\tau_p = \frac{F_{max}}{P_f L_e} \tag{1}$$

2.4 Fibre embedded length and perimeter measurement

The embedded interfacial area of each pull-out sample was characterised by measuring the embedded length and fibre perimeter. The embedded length was measured directly

on each polymer cylinder using a calliper. However, when characterising natural fibre properties, it is important to take into consideration the non-circular nature of their cross-section [28]. It has been shown that assuming an NF has a circular cross-section and calculating fibre properties based on diameter measurements from transverse observations can lead to significant error.

Once the samples had been tested, two pieces of the remaining free fibre were cut off and fixed to 250 g/m^2 card in a vertical position. These cards were then inserted into a mould that was subsequently filled with resin. Once set, the resin blocks were then ground and polished using progressively finer grinding papers for final cross-section and perimeter analysis, see Figure 10. Fibre cross-section was photographed using an Olympus GX51 microscope at different magnifications depending on the size of the fibre. For every picture, the cross-section was traced and exported for post-treatment as is illustrated in Figure 10. The resulting images were analysed by a macro-written for ImageJ. The macro-program converted each image file to a binary image and subsequently, after applying the respective scale, measured each area and perimeter by using the 'analyse particles' feature of ImageJ.

2.5 Controlled environment DMA fibre pull-out testing

Thomason and Yang have previously shown how a thermo-mechanical analyser can be modified to provide a well-controlled temperature environment in which to carry out interfacial strength testing using a microbond test [29,30]. Downes and Thomason further showed how a similar method could be adapted to carry out microbond testing in the temperature and humidity controlled environment of a dynamic mechanical analyser (DMA) [31]. In this section, we show how further modification of a DMA can enable pull-out testing of coir-PP samples can also be carried out in a similar temperature and humidity controlled environment.

A DMA Q800 from TA instruments was used in tension mode, to adapt the pull-out configuration that was previously illustrated in Figure 3, and which was used in the tests carried out at room temperature in the Instron tensile testing machine. The schematic diagram of the metallic frame that was developed to perform pull-out testing within the DMA, and test set-up are shown in Figure 11 (a) and Figures 11 (b). In the case of the DMA test, the position of the pull-out sample was opposite to the one used in the Instron test. The sample was placed in position, putting the fibre through the hole on the frame, and clamping the fibre at approximately 5 mm below the bottom surface of the plate in which the sample is positioned. Although not used in this study, the developed frame is also able to fit within the DMA humidity chamber, as illustrated in Figure 11 (c), which potentially enables investigating the effects of humidity on interfacial properties [31]. In the case of sub-ambient temperature testing a TA DMA gas cooling accessory was used.

The testing protocol that was developed, aimed to replicate the test on the Instron tensile testing machine. After the samples were in position and ready for testing, the DMA furnace was closed, and thereafter, equilibrated at the test temperature. This was followed by a 5 min isothermal segment, in order to ensure a constant equilibrium temperature in the sample. After that a strain ramp,

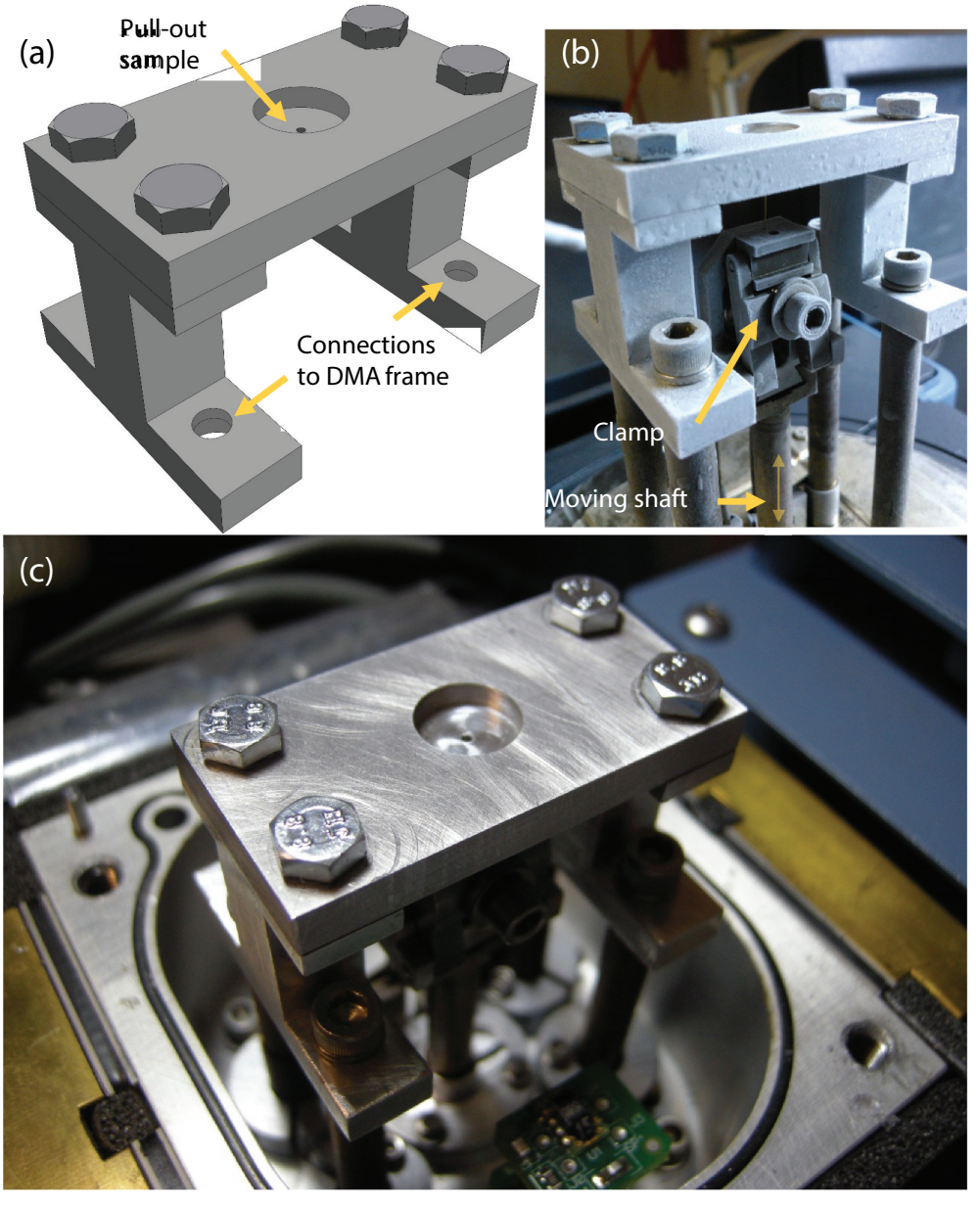

Figure 11. DMA pull-out frame. (a) Schematic drawing of the frame. (b) DMA set-up (picture taken after a test at – 40°C). (c) DMA pull-out frame fitted inside the DMA's humidity chamber.

equivalent to a displacement ramp of 0.5 mm/min, was applied to the fibre. The force-displacement curve was recorded by the TA software, and post-processed to find the peak debonding load. Once the peak force was obtained, the same process for measuring fibre perimeter and embedded length was applied as in the Instron pull-out method described above.

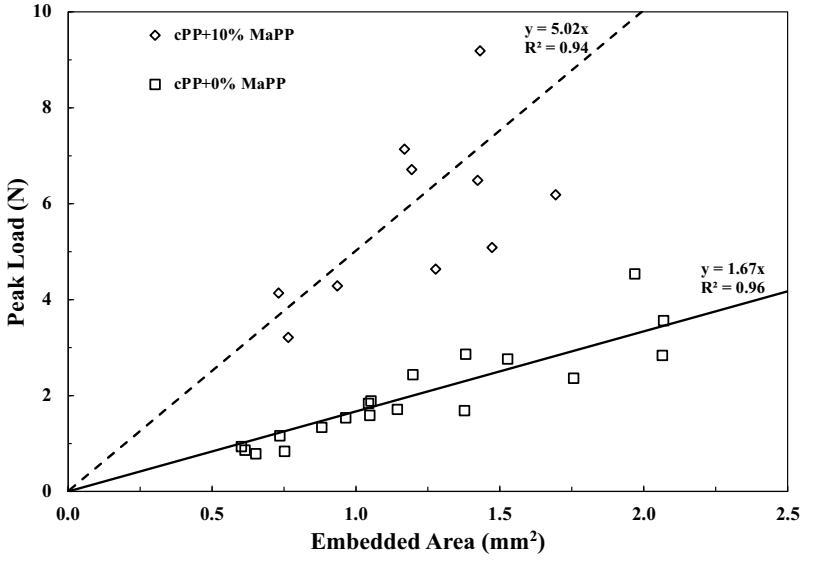

Figure 12. Peak load versus embedded area plots for pullout measurement with coir-cPP.

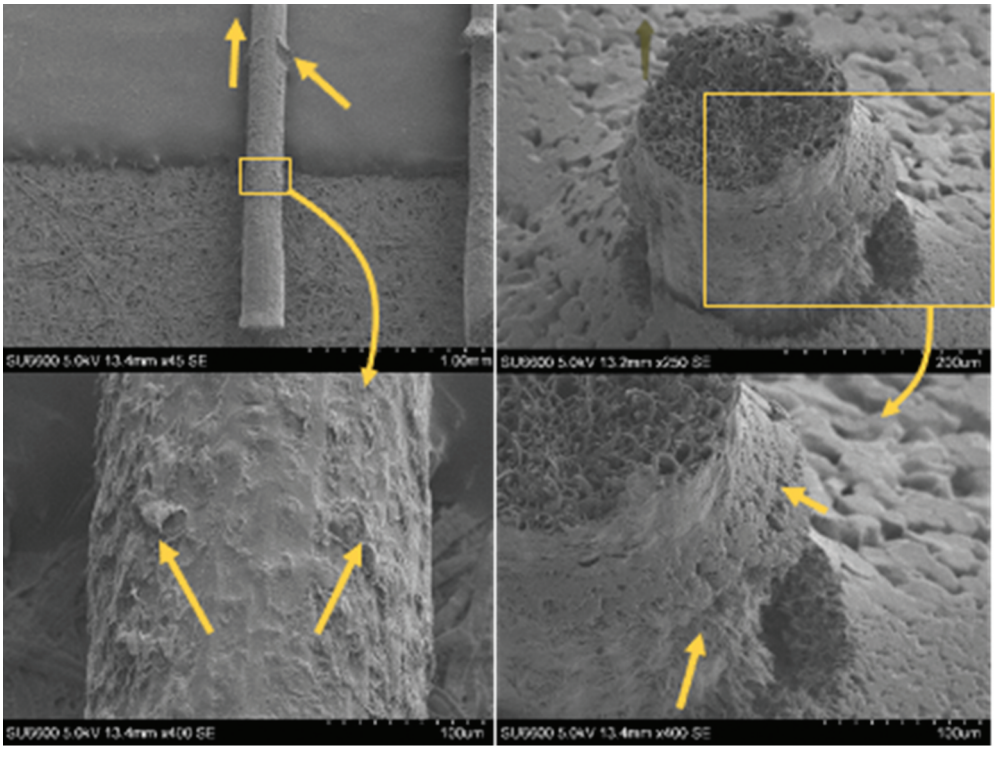

Figure 13. SEM examination of debonded cPP based samples. (a) (b) Coir fibre after being pulled out from a cPP+10 wt% MAPP sample. (c) (d) Failed pull-out test in which the fibre broke after it was partially pulled-out.

3. Results and discussion

Results of the room temperature Instron pull-out test of coir-cPP system and its respective variations in terms of MaPP content, carried out on the Instron machine at room temperature are illustrated in Figure 12. The value of the apparent IFSS for each system, is represented in the figure as the slope of the least-squares fitted straight line forced through the origin. From the R^2 values shown in the figure, and the individual data points, it can be seen that there is a clear scattering of the data. This relative scattering was observed to different extents with all the fibre-matrix combinations studied. Examples of the examination under the SEM of cPP-based pull-out samples, are shown in Figure 13. The investigation of the embedded surface area of debonded fibres revealed residual polymer and the existence of a polymer meniscus, which was especially evident at higher concentrations of MaPP (i.e. 5 and 10 wt%). In Figure 13 (b), it can be seen that remains of polymer stayed adhered to the fibre's surface after debonding. Detailed examination of this kind of fibre surfaces revealed that the remaining polymer was sheared in the direction of the pull-out force. Figure 13(c)andFigure13 (d)clearly illustrates, in a sample that failed while the fibre was being pulled-out, how the polymer meniscus remained adhered to the fibre, while residual polymer could also be seen on the pulled-out fibre surface.

The average IFSS obtained from the individual data point are listed in Table 1 along with their 95% confidence limits. In the case of coir-cPP a continuous increase of the apparent IFSS was observed for increasing MaPP content up to 10 wt%. It can also be noticed in Table 1 that the apparent IFSS of the coir-MaPP sample is equivalent to the average value of cPP+10% MaPP. In this case, a two sample t-test showed no significant difference at 95% confidence level (p-value = 0.88). Although the average apparent IFSS values are equivalent, close examination of the debonded areas of pure MaPP pull-out samples, revealed different post-debonded embedded area characteristics. Small polymer menisci were detected, but no observable residual polymer was found on the embedded area, as illustrated in Figure 14. This observation might indicate different debonding

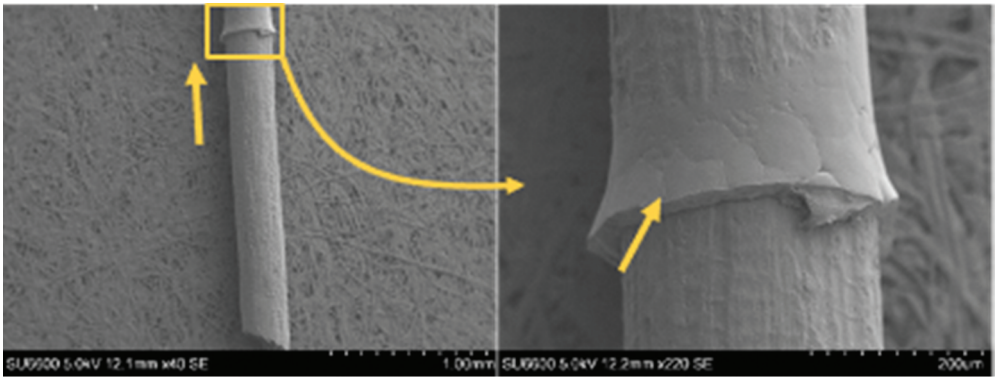

Figure 14. SEM examination of a typical debonded coir-MaPP sample.

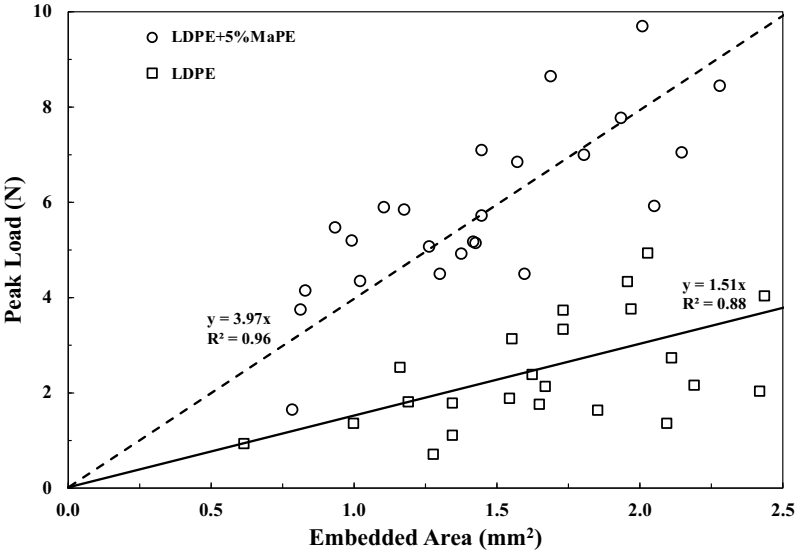

Figure 15. Peak load versus embedded area plots for pullout measurement with coir-LDPE.

behaviours in terms of how the crack propagates along the interface, and how the matrix might behave differently when subject to relatively high shear stresses due to the presence of a rubbery phase in the PP copolymer, which at the same time could lead to heterogeneous interaction between the matrix and the fibre.

Results of the pull-out test of coir-LDPE 1922SF system and its respective variation with a 5% MAPE content, carried out with the Instron machine at room temperature are illustrated in Figure 15. The value of the IFSS for each system, is represented in the figure as the slope of the least-squares fitted straight line forced through the origin. From the R-squared values showed in the figure, and the individual data points, it can be seen that there is a relatively high scattering of the data. As previously stated, this scattering has also been observed, to different extents, through all the previously analysed systems. A clear increase in the apparent IFSS is observed for the MaPE modified samples.

Three different temperatures were investigated using the DMA fibre pull-out set-up, −40°C, 20°C, and 100°C. Results of the pull-out tests of peak load versus embedded area of coir-hPP using the DMA and the Instron tensile testing machine at 20°C are compared in Figure 16. It can be seen that the two data sets strongly overlap and that the lines fitted according to Equation (1) have slopes which are very close. Although the values from the least-squares fit are a good indication of the comparability, the values from individual calculations (i.e. from each experimental point) were used to perform a series of two samples t-tests to compare both experimental results. The average value for the IFSS values obtained using the Instron was 3.2 MPa with a 95% CL of 0.46. The average value of the apparent IFSS obtained using the DMA was 3.5 MPa with a 95% CL of 0.68. The p value obtained from a two-tailed Student's t-Test was 0.13 indicating that the difference in average apparent IFSS values obtained using the two techniques was not significant at the 95% confidence level.

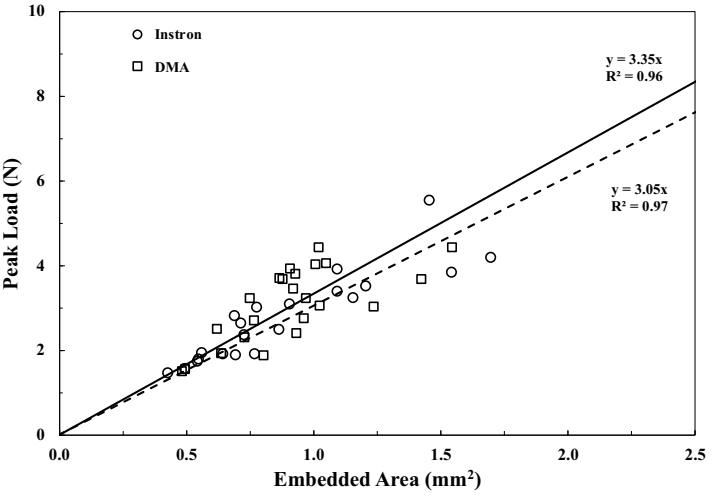

Figure 16. Comparison of peak load versus embedded area plots for coir-hPP obtained using Instron and DMA pullout setup.

The DMA pull-out results for peak load versus embedded area for coir-hPP at −40°C and 100°C are shown in Figure 17. Comparing the results obtained at room temperature in Figure 16 with these data, it can be seen that there is a clear dependency between the apparent IFSS and the testing temperature. This temperature dependence of IFSS has been reported for a number of other composite systems and is a result of the main contribution to the apparent IFSS being from residual radial compressive stresses at the fibre–matrix interface [29–31]. Based on the averages of the individual IFSS values it was observed that IFSS decreased from 5.2 MPa at −40°C to 3.5 MPa at 20°C and decreased further to only 1.7 MPa at 100°C. In all cases these differences in average IFSS values were significant at the 95% confidence level. Hence the developed technique for determining IFSS at different temperatures using a pull-out set-up in a DMA appears to be able to clearly discriminate a temperature effect on the measured level of interfacial adhesion in this fibre-matrix system.

Despite the continued high level of focus on the chemical nature of interfacial adhesion and interface modification, a number of authors have also commented on the role of shrinkage stresses contributing to the stress transfer capability at the fibre–matrix interface [11,29,30,32–37]. Thermoplastic composite materials are generally shaped at elevated temperature and then cooled. Since in most cases the thermal expansion coefficients of polymers are much greater than reinforcement fibres this cooling process results in compressive radial stress σ_R at the interface [32]. Assuming that the coefficient of static friction (μ_s) at the interface is non-zero then Coulombs friction law predicts that these compressive stresses will contribute a frictional component $\tau_f = \mu_s.\sigma_R$ to the apparent shear strength of the interface. In a series of recent publications [38] Thomason has examined the level of apparent IFSS in a large number of fibre-reinforced thermoplastic systems and shown clearly that the combination of components based on residual stress (σ_R) and physiochemical molecular interactions (τ_0) at the interface can then fully account for the measured IFSS using

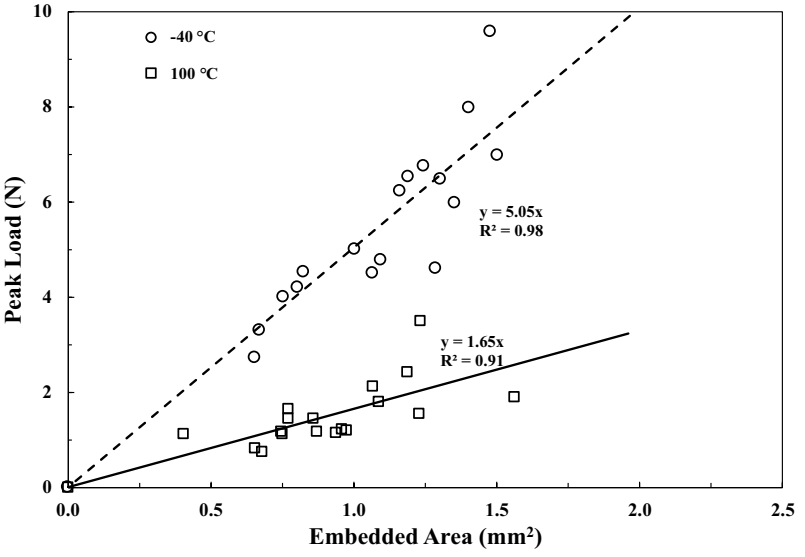

Figure 17. Peak load versus embedded area plots for coir-hPP obtained at different temperature in the DMA.

$$\tau_{app}(T) = \tau_0 + \mu_s \sigma_R(T) \tag{2}$$

where both τ_{app} and σ_R are functions of testing temperature [29].

It would appear from the foregoing discussion that a case can be made for residual thermal stresses contributing a significant amount to the temperature-dependent apparent IFSS measured in the coir-hPP system. Moreover, the relative proportion of this contribution is likely high in polyolefin based composites where the levels of other fibre–matrix physical and chemical interactions are low. The magnitude of these residual stresses can be adequately estimated using any of various model equations [32–35,39] which basically calculate the radial compressive strain developed at the fibre–matrix interface caused by the difference in the transverse thermal expansion coefficient of the fibre (α_{ft}) and the coefficient of linear thermal expansion of the polymer matrix (α_m) combined with the differential temperature between the IFSS testing temperature (T_t) and the temperature (T_0) below which these strains cannot relax away (normally taken as the crystallisation temperature of semi-crystalline polymer such as PP). This residual thermal strain can be converted into a radial compressive stress through the modulus of the polymer, which is also temperature dependent [39]. Hence

$$\sigma_R = \int_{T_0}^{T_t} \left(\alpha_m(T) - \alpha_{ft}(T)\right) E_m(T) dT \tag{3}$$

This radial compressive can then be converted into a contribution to the apparent IFSS through factoring in of the coefficient of static friction. Although values for the magnitude of μ_s in fibre-polymer systems are little reported or quantified in the literature, it should be clear that factors such as fibre surface roughness and the role of polymer wetting and interfacial interaction will be important in its determination. Consequently,

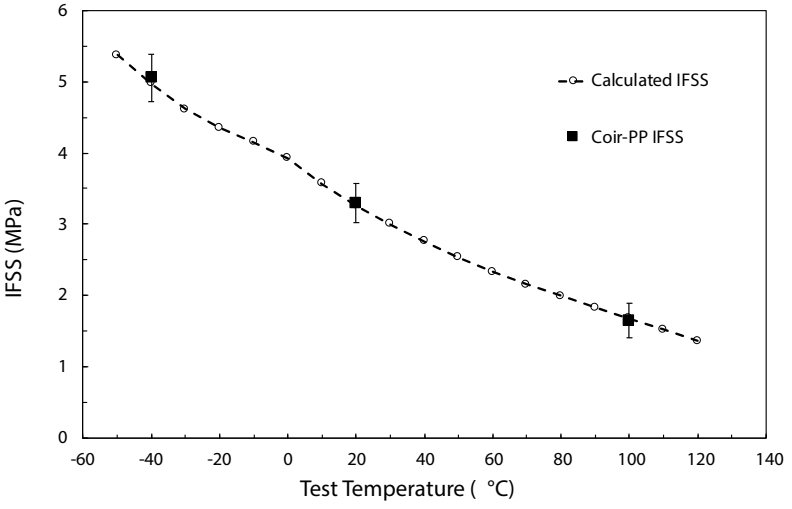

Figure 18. Comparison of coir-hPP experimental IFSS obtained at different temperatures compared to values calculated using Equation 2.

it may be that many of the chemical modifications applied to thermoplastic composites which are assumed to improve adhesion through increased chemical bonding across the interface may actually be changing the contribution of mechanical interlocking to the apparent adhesion by increasing the level of matrix-fibre wetting and consequently the static coefficient of friction.

Values for the temperature dependence of the modulus and expansion coefficient of the hPP used in this study have been reported previously [29]. Values for the transverse expansion coefficient of fibres are much more difficult to find although for the common manmade reinforcement such as glass and carbon their magnitude is so much smaller than that of the polymer matrix that their contribution can be reasonably ignored. However, that is not the case for natural fibres. There are even fewer values of α_{ft} for natural fibres available in the literature. Nevertheless, Thomason and Gentles have published values for the temperature dependence of α_{ft} for flax and sisal fibres [40]. Of these two, the internal structure of sisal matches better to that of coir and so we have used those values for the calculation of the residual interfacial thermal compressive stresses in the coir-hPP system at the three test temperatures used in this study. Similarly, values for μ_s are few and far between in the literature but Thomason has published a value of μ_s = 0.4 for jute fibres in the same hPP [11]. The values calculated using these input parameters in Equations 2 and 3 are compared with the temperature dependent IFSS values of the coir-hPP system in Figure 18. It can be seen that excellent agreement can be obtained between values calculated using Equation 2 and the experimental values of the IFSS of coir-hPP at different temperatures. This observation fits very well with the hypothesis that the measured value of IFSS in fibre reinforced thermoplastics is mainly derived from the combination of residual interfacial radial compressive stresses and static friction [38].

4. Conclusions

A method for sample preparation and testing of the interfacial shear strength of coir-thermoplastic systems has been presented and discussed. The sample preparation method described minimises the thermal degradation of both the natural fibre and the polymer matrix. Furthermore, a metallic frame was developed for an Instron tensile testing machine, which enabled the performing of pull-out testing at room temperature. Additionally, a metallic frame was also developed for a TA Q800 DMA. This enabled pull-out testing to be performed in a controlled atmosphere at various temperatures above and below room temperature.

Pull-out testing of coir-copolymer PP at room temperature, along with its respective MaPP modifications, revealed an overall trend in which the addition of MaPP led to higher apparent IFSS. A similar effect was found in the case of the coir-homopolymer PP system. In the coir-cPP system there was no significant increase in IFSS between 10% addition of MaPP and pure MaPP. The measured average apparent IFSS was 1.6 MPa for cPP, 4.9 MPa for cPP+10% MaPP and 5 MPa for coir-MaPP. An initial study of the interfacial properties of coir-LDPE system and its respective variation with a 5% MAPE content also revealed an increase of the apparent IFSS for the MAPE modified samples.

Table 1. IFSS values for Coir-cPP STS.

Matrix MaPP content (wt %)	IFSS in cPP (MPa)	95% Conf. limit
0	1.6	0.1
3	3.2	0.5
5	3.9	0.5
10	4.9	0.7
100	5.0	0.6

A procedure to characterise the temperature dependence of the interfacial properties of coir-homopolymer PP by modification of a dynamic mechanical analyser has also been presented and discussed. Good comparability between the room temperature pull-out data from the Instron tensile tester and the DMA machine was observed. The temperature dependence of the coir-hPP apparent IFSS showed high inverse dependency on the testing temperature. This observation fits well with the hypothesis that the measured IFSS in these natural fibre-thermoplastic composites is mainly due to the combination of residual interfacial radial compressive stresses and static friction.

Acknowledgments

The authors gratefully acknowledge the financial support of SABIC Petrochemicals B.V. and the EPSRC Doctoral Training Grant scheme.

Disclosure statement

No potential conflict of interest was reported by the author(s).

Funding

This work was supported by the Engineering and Physical Sciences Research Council; Saudi Basic Industries Corporation.

ORCID

James L. Thomason http://orcid.org/0000-0003-0868-3793

References

[1] Peças P, Carvalho H, Salman H, et al. Natural fibre composites and their applications: a review. J Compos Sci. 2018;2(4):66.
[2] Keya KN, Kona NA, Maraz KM, et al. Natural fiber reinforced polymer composites: history, types, advantages, and applications. Mater Eng Res. 2019;1(2):69–87.
[3] Ighalo JO, Adeyanju CA, Ogunniyi S, et al. An empirical review of the recent advances in treatment of natural fibers for reinforced plastic composites. Compos. Interfaces2020. DOI:10.1080/09276440.2020.1826274.
[4] Thomason JL. Why are natural fibers failing to deliver on composite performance? Proceedings of ICCM-17. Edinburgh UK; 2009. http://iccm-central.org/Proceedings/ICCM17proceedings/papers/D9.1%20Thomason.pdf
[5] Thomason JL, Rudeiros-Fernández JL. A review of the impact performance of natural fiber thermoplastic composites. Front Mater. 2018;5:60.
[6] Sahu P, Gupta M. A review on the properties of natural fibres and its bio-composites: effect of alkali treatment. Proc IMechE Part L: J Materials: Design Appl. 2020;234(1):198–217.
[7] Amiandamhen SO, Meincken M, Tyhoda L. Natural fibre modification and its influence on interfacial properties in biocomposite materials. Fibers Polym. 2020;21(4):677–689.
[8] Mohit H, Selvan VAM. A comprehensive review on surface modification, structure interface and bonding mechanism of plant cellulose fiber reinforced polymer based composites. Compos Interfaces. 2018;25(5–7):629–667.
[9] Thomason JL, Rudeiros-Fernández JL. Thermal degradation behaviour of natural fibres at thermoplastic composite processing temperatures. Polym Degrad Stab Accepted. 2021.
[10] Xie Y, Cas H, Xiao Z, et al. Silane coupling agents used for natural fiber/polymer composites: a review. Compos Part A Appl Sci Manuf. 2010;41(7):806–819.
[11] Thomason JL. Dependence of interfacial strength on the anisotropic fiber properties of jute reinforced composites. Polym Compos. 2010;31(9):1525–1534.
[12] Eichhorn SJ, Baillie CA, Mwaikambo LY, et al. Review: current international research into cellulosic fibers and composites. J Mater Sci. 2001;36(9):2107–2131.
[13] Hull D, Clyne TW. An introduction to composite materials. Cambridge University Press; 1996. Cambridge UK.
[14] Miller B, Muri P, Rebenfeld L. A microbond method for determination of the shear strength of a fiber/resin interface. Compos Sci Technol. 1987;28(1):17–32.
[15] Gaur U, Miller B. Microbond method for determination of the shear strength of a fiber/resin interface: Evaluation of experimental parameters. Compos Sci Technol. 1989;34(1):35–51.
[16] Zhou L-M, Kim J-K, Mai Y-W. On the single fibre pull-out problem: effect of loading method. Compos Sci Technol. 1992;45(2):153–160.
[17] Yue CY, Cheung WL. Interfacial properties of fibre-reinforced composites. J Mater Sci. 1992;27(14):3843–3855.
[18] Piggott MR.Why interface testing by single-fibre methods can be misleading. Compos. Sci. Technol. 1997;51:965–97.
[19] Beckert W, Lauke B. Critical discussion of the single-fibre pull-out test: does it measure adhesion? Compos. Sci Technol. 1998;57:1689–1706.

[20] Zhandarov SF, Pisanova EV. The local bond strength and its determination by fragmentation and pull-out tests. Compos Sci Technol. 1997;57(8):957–964.
[21] Piggott MR. Why the fibre/polymer interface can appear to be stronger than the polymer matrix. Compos Sci Technol. 1997;57(8):853–857.
[22] Ash JT, Cross WM, Svalstad D, et al. Finite element evaluation of the microbond test: Meniscus effect, interphase region, and vise angle. Compos Sci Technol. 2003;63 (5):641–651.
[23] Scheer RJ, Nairn JA. A comparison of several fracture mechanics methods for measuring interfacial toughness with microbond tests. J Adhes. 1995;53(1–2):45–68.
[24] Chou C, Gaur U, Miller B. The effect of microvise gap width on microbond pull-out test results. Compos Sci Technol. 1994;51(1):111–116.
[25] Lee CH, Khalina A, Lee SH. Importance of interfacial adhesion on characterization of plant-fiber-reinforced polymer composites: a review. Polymers. 2021;13(3):438.
[26] Yang L, Thomason JL, Zhu WZ. The influence of thermo-oxidative degradation on the measured interface strength of glass fibre-polypropylene Compos. Part A Appl Sci Manuf. 2011;42(10):1293–1300.
[27] Jlr F, Thomason JL, Soliman M. Characterisation of the mechanical and thermal degradation behaviour of natural fibres for lightweight automotive applications. In: Proceedings of ICCM-19. Montreal, Canada; 2013. http://www.iccm-central.org/Proceedings/ICCM19proceedings/papers/RUD81413.pdf
[28] Thomason JL, Carruthers J, Kelly J, et al. Fibre cross section determination and variability in sisal and flax and its effects on fibre performance characterisation. Compos Sci Technol. 2011;71(7):1008–1015.
[29] Thomason JL, Yang L. Temperature dependence of the interfacial shear strength in glass-fibre polypropylene composites. Compos Sci Technol. 2011;71(13):1600–1605.
[30] Thomason JL, Yang L. Temperature dependence of the interfacial shear strength in glass–fibre epoxy composites. Compos Sci Technol. 2014;96:7–12.
[31] Downes KA, Thomason JL. A method to measure the influence of humidity and temperature on the interfacial adhesion in polyamide composites. Compos Interfaces. 2015;22 (8):757–766.
[32] Nairn JA. Thermoelastic analysis of residual stresses in unidirectional, high-performance composites. Polym Compos. 1985;6(2):123–130.
[33] Di Landro L, Pegoraro M. Evaluation of residual stresses and adhesion in polymer composites. Compos Part A. 1996;27(9):847–853.
[34] Detassis M, Pegoretti A, Migliaresi C. Effect of temperature and strain rate on interfacial shear stress transmission in carbon/epoxy model composites. Compos Sci Technol. 1995;53 (1):39–46.
[35] Wagner HD, Nairn JA. Residual thermal stresses in three concentric transversely isotropic cylinders. Compos Sci Technol. 1997;57(9–10):1289–1302.
[36] Thomason JL. Interfacial strength in thermoplastic composites– at last an industry friendly measurement method? Compos Part A. 2002;33(10):1283–1288.
[37] WenBo L, Shu Z, LiFeng H, et al. Interfacial shear strength in carbon fiber-reinforced poly (phthalazinone ether ketone) composites. Polym Compos. 2013;34(11):1921–1926.
[38] Thomason JL, Yang L, Minty RF. Are silanes the primary driver of interface strength in glass fibre composites? Exploring the relationship of the chemical and physical parameters which control interfacial strength. In: Proceedings of ECCM-18. Athens, Greece; 2018. https://az659834.vo.msecnd.net/eventsairwesteuprod/production-pcoconvin-public/8aba9d8408894ec6bb3a538f261bb6e2
39 Piggott MR. Load-bearing fibre composites. Oxford: Pergamon Press; 1980.
[40] Thomason JL, Yang L, Gentles F. Characterisation of the anisotropic thermoelastic properties of natural fibres for composite reinforcement. Fibers. 2017;5:36. 2017.